Available online at www.sciencedirect.com
SCIENCE DIRECT®
Journal of the European Ceramic Society 26 (2006) 343–349
www.elsevier.com/locate/jeurceramsoc

Prediction of crack deflection in porous/dense ceramic laminates

D. Leguillon[a,*], S. Tariolle[b], E. Martin[c], T. Chartier[d], J.L. Besson[d]

[a] *LMM, CNRS UMR7607, Université P. et M. Curie, case 162, 4 place Jussieu, 75252 Paris Cedex 05, France*
[b] *CES, CNRS UMR 5146, Ecole des Mines de Saint-Etienne, St Etienne, France*
[c] *LCTS, CNRS UMR 5801, Université Bordeaux 1, Pessac, France*
[d] *SPCTS, CNRS UMR 6638, E.N.S. de Céramiques Industrielles, Limoges, France*

Received 24 June 2004; received in revised form 4 November 2004; accepted 12 November 2004
Available online 19 January 2005

Abstract

The arrangement of ceramic layers in laminated structures is an interesting way to enhance the flaw tolerance of brittle ceramic materials. The interfaces are expected to deflect cracks, increasing the fracture energy of the laminate compared to a monolithic material and thus raising the toughness.

Laminates have been fabricated with alternating dense and porous layers of the same material, i.e. SiC or B_4C, in order to obtain a good chemical compatibility between the laminas and almost no thermal residual stresses. Porosity, in the porous layers, is achieved by incorporating organic particles which are removed during the debinding step. In this context, the target of this study is to predict the volume fraction of pores, in the porous layer, required to cause crack deflection.

The proposed criterion derives from an energy balance. It relies on a two-scale analysis taking into account the laminated structure of the material. It can be written in terms of two relevant material parameters: the ratio of Young's moduli of the dense and porous materials and toughness ratios. A unique function depending on the volume fraction of pores can be used to express the two above-mentioned ratios. Assuming a cubic lattice of spherical voids, the parameters of the porous ceramic depend linearly on the porosity and vanish at the point of percolation of pores. As a consequence, the criterion can be rewritten in term of a single parameter: the porosity.

Crack deflection is permitted only for very high values of the porosity. Predicted values agree satisfactorily with experiments on SiC and B_4C. The comparison with the He and Hutchinson criterion shows that this latter underestimates the correct value.

Keywords: Fracture; Toughness and toughening; Laminates; Porosity

1. Introduction

Laminated structures with weak interfaces or interphases constitute one strategy to improve the flaw tolerance of brittle ceramic materials. These structures have proved to be efficient in increasing fracture energy by promoting crack deflection mechanisms at interfaces between layers: cracks that form in one layer are deflected along the interface with adjacent layers which increases the fracture energy of the laminate compared to that of a monolithic material and thus raises the apparent toughness. Laminar ceramic composites are generally fabricated by stacking layers of different compositions in a suitable sequence.[1] Alternating dense and porous layers of the same material offers the best chemical compatibility and almost no thermal residual stresses. Crack deflection has been observed within such systems as the result of the presence of porous interlayers.[2–9] The question is thus to predict the volume fraction of pores, in the porous layers, required to cause crack deflection.

Two kinds of ceramic laminates are analysed: silicon carbide (SiC)[2–7] and boron carbide (B_4C).[7,8] The specimens are fabricated by stacking layers obtained by tape-casting, and then by lamination, debinding and sintering. Porosity of porous layers is introduced by adding pore-forming agents such as corn starch or polymer particles. These organic par-

* Corresponding author. Tel.: +33 144 275 322; fax: +33 144 275 259.
E-mail address: dol@ccr.jussieu.fr (D. Leguillon).

0955-2219/$ – see front matter © 2004 Elsevier Ltd. All rights reserved.
doi:10.1016/j.jeurceramsoc.2004.11.003

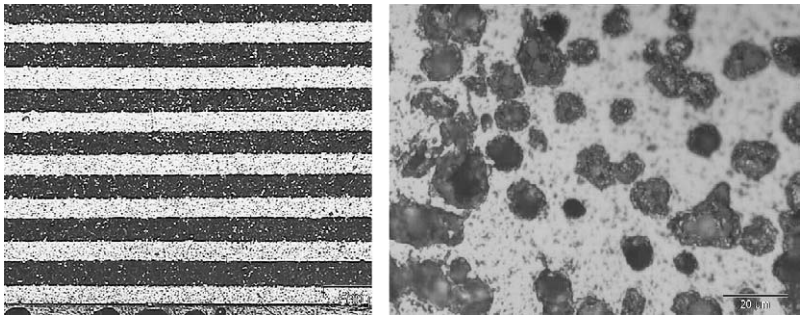

Fig. 1. Macrostructure of boron carbide composite with interlayers obtained by the use of corn starch (left), microstructure of porous boron carbide obtained with 20 vol.% of corn starch (right).

ticles are burned out during the debinding step, prior to sintering. Dense and porous layers have the same thickness after sintering ($e \approx 100\ \mu m$). Laminated specimens made of 20 layers have been tested under 3-point flexure loading. Details on the fabrication of specimens and the measurement of elastic and failure parameters can be found in Reynaud and co-workers[5,6] and in Tariolle et al.[7,8] Fig. 1 shows micrographs of the layered B_4C materials and depicts the pore shapes within the porous interlayers.[8]

The analyses of crack deflections by interfaces are generally based on two models due to He and Hutchinson.[10,11] Both are carried out in an unbounded domain made of two elastic materials. In the first one,[10] the primary crack lies in one material and impinges on the interface. Two virtual crack extensions are considered, either deflected along the interface (Fig. 2b) or straight in the adjacent layer. The energy release rates at the tip of these two extensions are compared. The drawback of this approach is the arbitrary choice of the two increment lengths. In the second He and Hutchinson model,[11] the primary crack is along the interface and the ability of the crack to kink out of the interface is studied. The two criteria involve the toughness of the materials and of the interface. Curiously, it is often this second paper that is used to interpret the experimental results of cracks deflection in ceramic laminates, although the main assumption, a long primary interface crack, is not fulfilled. Moreover, in any case, it is clear from Fig. 2b that the laminated environment of the crack tip is ignored in these approaches.

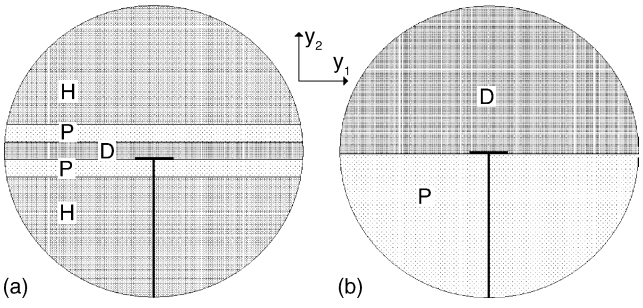

Fig. 2. Schematic view of the inner (unbounded) stretched domain for a deflection at a porous/dense interface: (a) the present analysis (P: porous, D: dense, H: homogenized); (b) He and Hutchinson approach.[10]

The present model relies on a two-scale analysis where the laminated structure is taken into account as explained in Section 2. The criterion proposed in Section 3 derives from an energy balance and can take into account a complementary stress criterion. This makes it possible to avoid the above-mentioned drawback, since virtual crack extension lengths are known. The criterion is expressed in terms of two relevant parameters: the Young's moduli and toughness ratios of the dense and porous layers. In Section 4, experiments show that these ratios can be written quite simply as functions of the porosity. Sections 5 and 6 are devoted to the study of the crack deflection at the dense/porous and porous/dense interfaces. A short Section 7 is dedicated to the analysis of the role of the relative thickness of porous layers. Section 8 deals with the minor influence of Poisson's ratios.

2. The asymptotics of the problem

The model is based on a two-scale analysis, the small parameter being the layers thickness. At the macro scale the laminated micro-structure is ignored, as a first approximation, the whole laminate is treated as a homogeneous material. It is homogenized using a rule of mixture for simplicity, since more sophisticated homogenization processes do not bring significant differences in the final results.[12] There is a primary crack for which the tip undergoes the classical mode I singular field. The antisymmetric mode II is inhibited due to the symmetries.

Within this framework, the displacement solution (so-called far field) prior to any crack growth can be written in plane elasticity:

$$\underline{U}^0(x_1, x_2) = \underline{U}^0(0, 0) + k_I \sqrt{r}\, \underline{u}_I(\theta) + \cdots \tag{1}$$

Here x_1 and x_2 stand for the Cartesian coordinates and r and θ for the polar ones. The coefficient k_I is the stress intensity factor and the angular shape function is denoted $\underline{u}_I(\theta)$.

Considering now a small crack extension ℓ, the perturbed solution is expressed as a correction brought to the initial term (Eq. (1)):

$$\underline{U}^\ell(x_1, x_2) = \underline{U}^0(x_1, x_2) + \text{small correction} \tag{2}$$

The small correction is assumed to vanish as $\ell \to 0$.

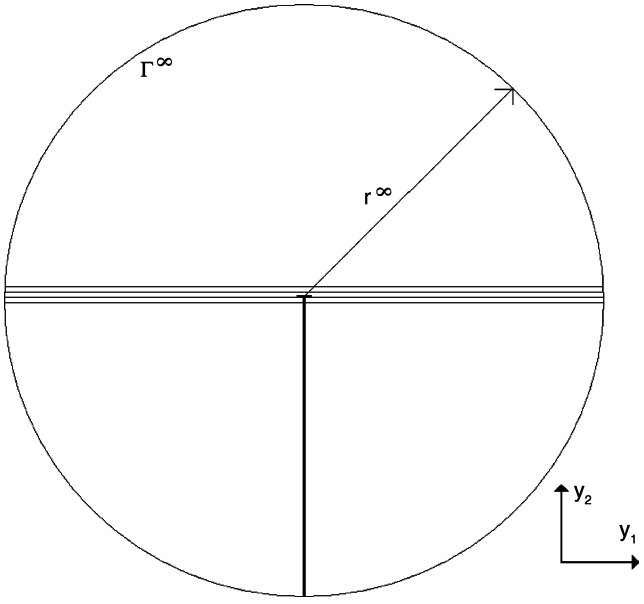

Fig. 3. The inner stretched domain and its artificial outer boundary Γ^∞. The origin is located at the tip of the primary crack (i.e. before branching).

The micro scale is obtained by stretching the domain around the primary crack tip by $1/e$, e being the layer thickness. Considering the limit $e \to 0$, the problem is now settled in an unbounded domain, so-called inner domain. In order to have tractable computations, this domain is artificially bounded at a large distance ($r^\infty \gg 1$, where r^∞ is the radius of the artificial boundary and 1 the dimensionless stretched thickness of the layers, say $r^\infty = 200$ for instance, see Fig. 3) from the primary crack tip. Moreover, only few dense (D in Fig. 2a) and porous (P in Fig. 2a) layers, say 3 or 4, are kept in the vicinity of the primary crack tip, the remaining part being replaced by the homogenized material (H in Fig. 2a). The validity of this simplification will be discussed in Section 3.

Using the change of variable $y_i = x_i/e$ ($\rho = r/e$), $\underline{U}^0$ can be expanded as (near field):

$$\begin{aligned}\underline{U}^0(x_1, x_2) &= \underline{U}^0(ey_1, ey_2)\\ &= \underline{U}^0(0,0) + k_I\sqrt{e}\,\underline{W}(y_1, y_2, 0) + \cdots\end{aligned} \tag{3}$$

where the 0 in $\underline{W}$ recalls that in a first step there is no crack extension. The function $\underline{W}$ is the solution to the following problem:

$$\begin{cases} -\nabla_y \cdot \sigma = 0 \\ \sigma = C : \nabla_y \underline{W} \\ \sigma \cdot \underline{n} = 0 \text{ along the crack faces} \\ \underline{W} \text{ behaves like } \sqrt{\rho}\,\underline{u}_I(\theta) \text{ at infinity} \end{cases} \tag{4}$$

The first equation is the balance of momentum (equilibrium). The symbol nabla ∇_y holds for derivatives with respect to y_1 and y_2. The second equation is the constitutive law, C is the elastic operator, it takes different values in the dense and porous layers and in the homogenized remaining part. The third equation expresses that the crack faces are free of traction. Finally, the last one is the matching condition with the mode I term involved in the far field (Eq. (1)).

Similarly, a crack extension ℓ either in the next layer or along the interface (a deflection at the interface porous/dense is illustrated in Fig. 2a) leads to the following expansion:

$$\begin{aligned}\underline{U}^\ell(x_1, x_2) &= \underline{U}^{e\mu}(ey_1, ey_2)\\ &= \underline{U}^0(0,0) + k_I\sqrt{e}\,\underline{W}(y_1, y_2, \mu) + \cdots\end{aligned} \tag{5}$$

where $\mu = \ell/e$ is the dimensionless crack extension length. Here $\underline{W}$ must fulfil the same system of equations (Eq. (4)), the traction free condition (Eq. (4_3)) being extended to the faces of the new extension of the crack.

3. The deflection criterion

Within this framework, the leading term of the change in potential energy between the two states (prior to and following a crack extension) is written:[13]

$$\delta W = k_I^2 \left[A\left(\frac{E_\mathrm{p}}{E_\mathrm{d}}, \mu\right) - A\left(\frac{E_\mathrm{p}}{E_\mathrm{d}}, 0\right)\right] ed \tag{6}$$

where d stands for the specimen depth (plane elasticity). E_d and E_p are respectively the Young's moduli of the dense and the porous ceramics. Poisson's ratios play a minor role as shown below in Fig. 12. The function A is numerically derived from the displacement field $\underline{W}$ using a contour integral:[13,14]

$$A\left(\frac{E_\mathrm{p}}{E_\mathrm{d}}, \mu\right) = \psi(\underline{W}(y_1, y_2, \mu), \sqrt{\rho}\,\underline{u}_I(\theta)) \tag{7}$$

with

$$\psi(\underline{U}, \underline{V}) = \frac{1}{2}\int_\Gamma (\sigma(\underline{U})\underline{n}\,\underline{V} - \sigma(\underline{V})\underline{n}\,\underline{U})\,\mathrm{d}S$$

Γ is any contour in the inner domain surrounding and located far from the crack tip and its extension, $\underline{n}$ is its normal pointing toward the crack tip. For practical reasons, the outer artificial boundary Γ^∞ is selected (see Fig. 3). The integral ψ in Eq. (7) is contour independent for any $\underline{U}$ and $\underline{V}$ fulfilling the equilibrium equation (Eq. 4_1).

A necessary condition for the crack growth is a consequence of an energy balance:

$$\delta W \geq G^c \ell d \Rightarrow k_I^2 f\left(\frac{E_\mathrm{p}}{E_\mathrm{d}}, \mu\right) \geq G^c \tag{8}$$

with

$$f\left(\frac{E_\mathrm{p}}{E_\mathrm{d}}, \mu\right) = \frac{A(E_\mathrm{p}/E_\mathrm{d}, \mu) - A(E_\mathrm{p}/E_\mathrm{d}, 0)}{\mu}$$

Here G^c is the toughness in the direction of fracture and ℓd is the newly created crack surface. This expression (Eq. (8)) must be considered twice, once for a deflection (index def in the following) and once for a penetration in the next layer

(index pen). Deflection is promoted if the above inequality holds true for deflection but is wrong for penetration, it leads to:

$$\frac{f_{\rm def}(E_{\rm p}/E_{\rm d},\mu_{\rm def})}{f_{\rm pen}(E_{\rm p}/E_{\rm d},\mu_{\rm pen})} \geq \frac{G^c_{\rm def}}{G^c_{\rm pen}} \tag{9}$$

where $G^c_{\rm pen}$ and $G^c_{\rm def}$ are the toughness of the next layer (penetration mechanism) and of the interface (deflection mechanism). It will be assumed in the following that the toughness of the interface is that of the porous material. Indeed, if the interface was stronger then the crack would grow within the porous medium at a short distance from the interface. Such a choice is also suggested in Fujita et al.[15]

Clearly the dimensionless crack increment lengths $\mu_{\rm def}$ and $\mu_{\rm pen}$ play a role in the above relation. Now we make the following reasonable additional assumption: if the crack penetrates the next layer then it breaks it completely: $\ell_{\rm pen} = e \Rightarrow \mu_{\rm pen} = 1$. The deflected extension length remains to be determined. It could be done using a maximum stress criterion.[13] For simplicity, we assume here:

$$\mu_{\rm def} = \mu_{\rm pen} = 1 \tag{10}$$

This choice is less arbitrary than that of He and Hutchinson[11] since it refers to a characteristic length of the microstructure (the layer thickness) that does not exist in their approach (Fig. 2a and b). Nevertheless, complete computations relying on a stress criterion have been carried out and it has been observed that the deflection length increases with the porosity but that the final results are not deeply modified.[12,16]

Finally the criterion takes the simplified form:

$$g\left(\frac{E_{\rm p}}{E_{\rm d}}\right) \geq \frac{G^c_{\rm def}}{G^c_{\rm pen}} \tag{11}$$

with

$$g\left(\frac{E_{\rm p}}{E_{\rm d}}\right) = \frac{A_{\rm def}(E_{\rm p}/E_{\rm d},1) - A(E_{\rm p}/E_{\rm d},0)}{A_{\rm pen}(E_{\rm p}/E_{\rm d},1) - A(E_{\rm p}/E_{\rm d},0)} \tag{12}$$

It is clear from this expression that the crucial point is the knowledge of two relevant data: the ratios of the elastic and toughness parameters. They can be expressed in terms of the porosity as proposed in the next section.

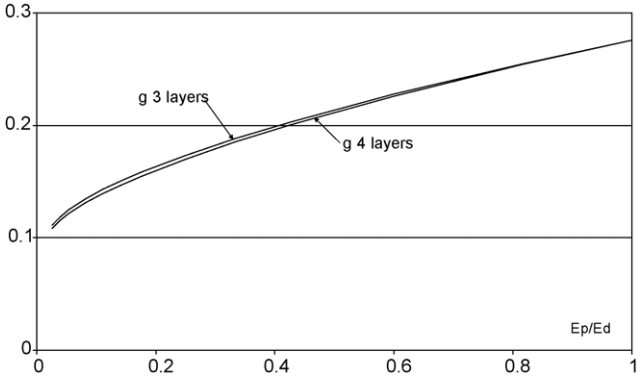

Fig. 4. The function g (Eq. (12)) (solid lines) vs. the Young's moduli ratio $E_{\rm p}/E_{\rm d}$ for two models of geometry (3 and 4 layers) at the porous/dense interface.

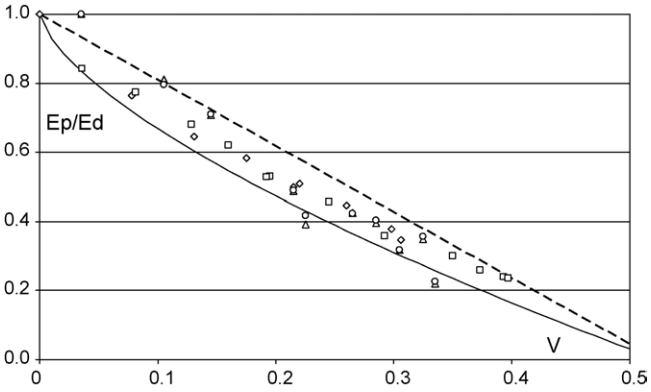

Fig. 5. Young's moduli ratio vs. pore volume fraction V: SiC with Polyamide particles[5–7] (diamonds), SiC with corn starch particles[3,7,8] (squares), B_4C with corn starch particles[7,8] (triangles). Shear modulus ratio vs. pore volume fraction V: B_4C with corn starch particles[8] (circles). The dashed line is the function $H(V)$ (Eq. (13)), the solid line is the function $K(V)$ (Eq. (14)).

A simplification of the geometry of the inner domain (Figs. 2a and 3) has been used. Only three or four layers have been considered around the crack tip, the remaining part of the material being replaced by a homogenized (averaged) one. Fig. 4 compares the function g defined in Eq. (12) when 3 and 4 layers are kept around the crack tip. Obviously, the simplified geometry retained in this model seems to be sufficient to our purpose.

4. Elastic and fracture parameters of the porous ceramic

The two Figs. 5 and 6 show that a unique function depending on the volume fraction of pores V can be used to express the elastic and fracture parameters of the porous material. In the first case (Eq. (13)) the parameters depend linearly on the volume fraction of pores V, whereas they depend linearly on

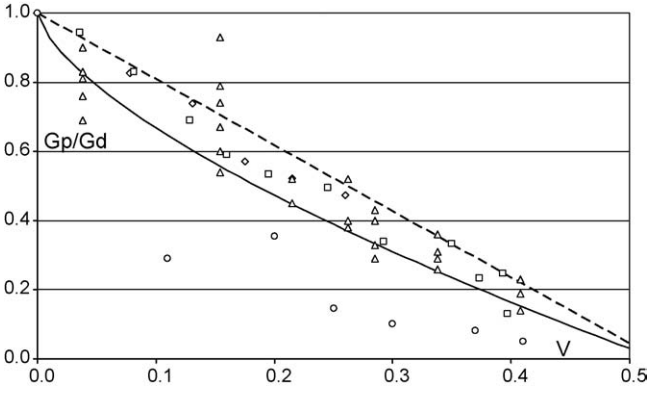

Fig. 6. Toughness ratio vs. pore volume fraction V: SiC with polyamide particles[5–7] (diamonds), SiC with corn starch particles[3,7,8] (squares), B_4C with corn starch particles[7,8] (circles), SiC with PTFE particles[3] (triangles). $H(V)$ (Eq. (13)) dashed line, $K(V)$ (Eq. (14)) solid line.

the largest surface fraction of pores S in the second case (Eq. (14)):

$$E_p = H(V)E_d; G_p^c = H(V)G_d^c \quad \text{with}$$

$$H(V) = 1 - \frac{6V}{\pi} \tag{13}$$

or

$$E_p = K(V)E_d; G_p^c = K(V)G_d^c \quad \text{with}$$

$$K(V) = 1 - \frac{4S}{\pi} = 1 - \left(\frac{6V}{\pi}\right)^{2/3} \tag{14}$$

where G_p^c and G_d^c are the toughness respectively of the porous and the dense ceramics.

In both cases a cubic lattice of spherical voids is assumed and the parameters of the porous ceramic vanish at the percolation condition of pores ($V = \pi/6 = 0.52$). Such a choice is consistent with the process used to create porosity by addition of spherical pyrolysable particles of constant diameters.[2–8] Higher volume fraction of pores can be obtained using particles of different sizes.[9]

It must be pointed out that, throughout this paper, the term "dense" is related to the stiffer material. The sintering leads to a residual close porosity in the bulk (2.5% in SiC and 6% in B_4C) independent of that obtained by addition of pore forming agents. This residual porosity is formed of pores much smaller than those resulting from the addition of particles. It can be ignored in the present analysis but has to be taken into account in the measures:

$$V = \tilde{V} - V_0 \tag{15}$$

where $\tilde{V}$ is the actual porosity and V_0 the initial (residual) one if no pore forming agent is added.

As a consequence of Eqs. (13) and (14), the deflection criterion (Eq. (11)) can be rewritten:

$$h(V) \geq H(V) \quad \text{with} \quad h(V) = g\left(1 - \frac{6V}{\pi}\right) \tag{16}$$

or

$$k(V) \geq K(V) \quad \text{with} \quad k(V) = g\left(1 - \left(\frac{6V}{\pi}\right)^{2/3}\right) \tag{17}$$

The two following Figs. 5 and 6 exhibit experimental measures of the Young's moduli and the toughness ratios for the two types of laminates and different additional pore forming agents: corn starch, polyamide and PTFE. Data are taken from Blanks et al.,[3] Reynaud and co-workers[5–7] and Tariolle et al.[7,8] In both cases the better matching is obtained using the surface fraction of pores (Eq. (17)) (dashed lines).

5. Deflection at the dense/porous interface

In this case, the so-called next layer is a porous one and the toughness ratio in Eq. (9) or Eq. (11) equals 1[15]

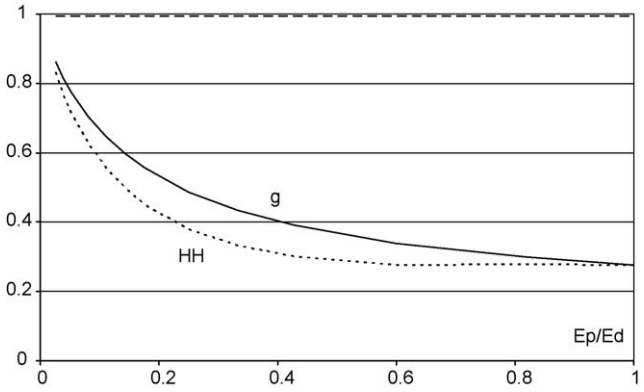

Fig. 7. The function g (Eq. (12)) (solid line) vs. the Young's moduli ratio E_p/E_d and the He and Hutchinson approach[10] (HH, dotted line) compared to the toughness ratio G_p^c/G_d^c (dashed line) at the dense/porous interface.

(see Section 3):

$$G_{def}^c = G_{pen}^c = G_p^c \tag{18}$$

The function g (Eq. (12)) (solid line) and the toughness ratio (dashed line) are plotted versus the Young's moduli ratio (Fig. 7). As expected, this figure shows clearly that no deflection can occur at such an interface, since the inequality (Eq. (11)) never holds true. The He and Hutchinson (HH) approach[10] is also plotted (dotted line) and leads to the same conclusion.

6. Deflection at the porous/dense interface

The so-called next layer is now a dense one. The function g (Eq. (12)) and the toughness ratio are again plotted versus the Young's moduli ratio (Fig. 8) at a porous/dense interface. It is only assumed that the two ratios (Young's moduli and toughness) follow the same rule (whatever this rule, i.e. Eqs. (16) and (17) or any other). The toughness ratio in Eq. (11)

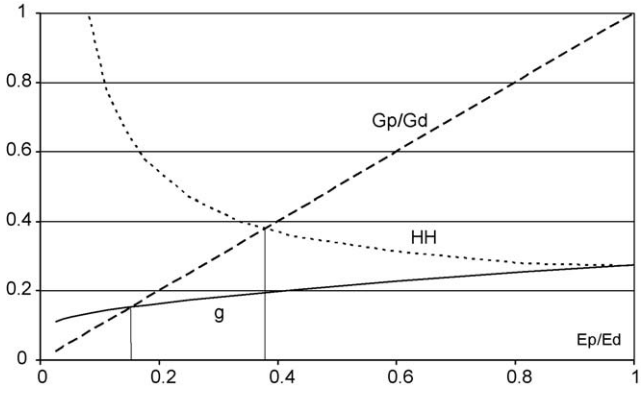

Fig. 8. The function g (Eq. (12)) (solid line) vs. the Young's moduli ratio E_p/E_d and the He and Hutchinson approach[10] (HH, dotted line) compared to the toughness ratio G_p^c/G_d^c (dashed line) at the porous/dense interface.

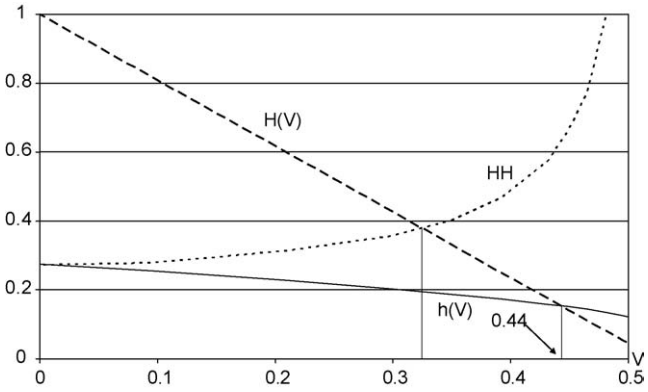

Fig. 9. The function h (Eq. (16)) (solid line) vs. the volume fraction of pores and the He and Hutchinson approach[10] (HH, dotted line) compared to the toughness ratio $H(V) = G^c_p/G^c_d$ (Eq. (13)) (dashed line).

is:

$$\frac{G^c_{def}}{G^c_{pen}} = \frac{G^c_p}{G^c_d} \tag{19}$$

The answers brought by the present analysis and the He and Hutchinson one[10] differ now significantly, the agreement with the experiments will be discussed below.

The criterion can be also plotted versus the volume fraction of pore V. It is illustrated in the two following figures derived from the single Fig. 8. In the first one (Fig. 9), the elastic and fracture parameters depend linearly on the volume fraction of pores (Eq. (16)), whereas in the second (Fig. 10) they depend linearly on the surface fraction of pores (Eq. (17)). Clearly the predicted porosity that causes crack deflection (arrows in Figs. 9 and 10) is above 40% in both cases. If one does not forget the residual porosity in the sintered parts (Eq. (15)), these results are in a good agreement with the experiments of Reynaud and co-workers[7,8] and Tariolle[8,9] while the He and Hutchinson approach[10] underestimates it. Blanks et al.[3] found a wide range of values: between 34% and 44%. Below 34% no deflection was observed, above 44% an extensive deflection was obtained (this last value is in agreement with

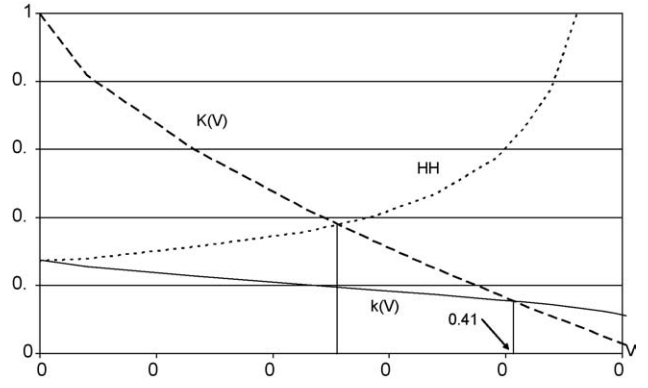

Fig. 10. The function k (Eq. (17)) (solid line) vs. the surface fraction of pores and the He and Hutchinson approach[10] (HH, dotted line) compared to the toughness ratio (Eq. (14)) $K(V) = G^c_p/G^c_d$ (dashed line).

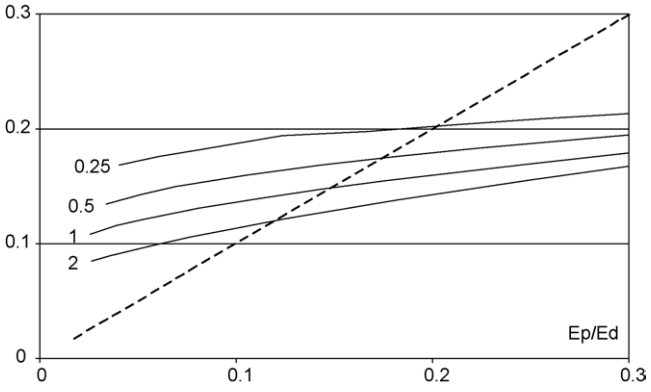

Fig. 11. The function g (Eq. (12)) (solid line) vs. the Young's moduli ratio E_p/E_d for different thicknesses ratio e_p/e_d (0.25, 0.5, 1, 2) compared to the toughness ratio G^c_p/G^c_d (dashed line) at the porous/dense interface.

the present analysis). Between the two values, the primary crack changes direction but kinks out immediately. In this latter case, the work of fracture is not strongly increased, the design goal is not attained.

7. The influence of the porous layers thickness

Throughout this paper, the porous material is considered as homogenous, this implies that the pores size is much smaller than the layers thickness. This property must not be forgotten, especially in this section. The porous layers thickness can be diminished provided it does not interfere with the pores diameter. Typically, at least one decade must separate these two characteristic lengths, the ratio between the pore diameter and the layer thickness must not exceed 0.1.

Numerical results show that thin porous layers tend to promote crack deflection. In Fig. 11 (a zoom of Fig. 8 in the range 0–0.3 for E_p/E_d), the function g (Eq. (12)) is plotted versus the Young's moduli ratio E_p/E_d for different values of the thicknesses ratio e_p/e_d, where e_p and e_d are respectively the porous and dense layer thicknesses. Results are summarized in Table 1. The model of porosity relies on function H defined in Eq. (12). The porosity required to promote deflection decreases with the porous layers thickness. Nevertheless, this effect remains small, the reduction is only about 10% when the relative porous layers thickness is divided by 8.

8. The influence of the Poisson's ratios

The Poisson's ratios of the components have been omitted in the above discussion. The next figure shows that they play

Table 1
Young's moduli ratio E_p/E_d and pore volume fraction V promoting crack deflection for various porous/dense layers thickness ratios e_p/e_d

e_p/e_d	2	1	0.5	0.25
E_p/E_d	0.120	0.150	0.175	0.205
V	0.461	0.445	0.432	0.416

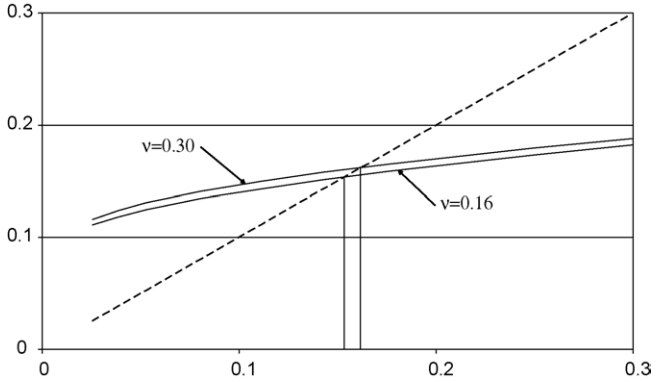

Fig. 12. The function g (Eq. (12)) (solid lines) vs. the Young's moduli ratio E_p/E_d for two different Poisson's ratio compared to the toughness ratio G_p^c/G_d^c (dashed line) at the porous/dense interface.

a minor role. It is assumed that both dense and porous ceramics have the same Poisson's ratio. Two values are compared in Fig. 12: $\nu = 0.16$ (B_4C) (note that $\nu = 0.17$ for SiC) and a realistic value met in many materials $\nu = 0.3$. Clearly the deviation in Young's moduli ratio causing deflection is weak (<6%) (Fig. 12). Using the porosity function H (Eq. (13)), it leads to about 1% deviation in the pore volume fraction V. It is obviously a negligible effect.

9. Conclusion

The first conclusion to draw is that deflection is very difficult to promote by porous layers obtained by the addition of spherical pore forming particles. This prediction correlates well with experimental results: Reynaud and coworkers[5–7] did not observe any extensive deflection in SiC below $\tilde{V} = 42\%$ (i.e. $V \approx 40\%$) and Tariolle et al.[7,8] found a significant deflection for a rather high value $\tilde{V} = 52\%$ (i.e. $V \approx 46\%$) in B_4C. It is in a good agreement with the present model, while the one based on the second He and Hutchinson approach,[11] as proposed by Clegg et al.,[2–4] tends to significantly underestimate the experimental values. The other well-known He and Hutchinson approach[10] neglects the laminated micro-structure of the material and gives an erroneous low value of the porosity causing crack deflection.

Finally, emphasis must be put on Figs. 7 and 8 that are in a way intrinsic, porosity does not occur explicitly. They play the role of 'master curves' and can be used whatever the dependence of the elastic and fracture properties on the porosity. The only assumption is that the Young's modulus and the toughness of the porous material follow the same rule. This may be wrong for small porosity values. But the present analysis deals only with large values of the porosity that can cause crack deflection, for which the assumption seems to be valid.

Acknowledgement

This work was supported by the French Ministry of Research in the ACI program "Surfaces and Interfaces 2001–2003".

References

1. Chartier, T., Merle, D. and Besson, J. L., Laminar ceramic composites. *J. Eur. Ceram. Soc.*, 1995, **15**, 101–107.
2. Clegg, W. J., Blanks, K. S., Davis, J. B. and Lanckmans, F., Porous interfaces as crack deflecting interlayers in ceramic laminates. *Key Eng. Mater.*, 1997, **132–136**, 1866–1869.
3. Blanks, K. S., Kristofferson, A., Carlström, E. and Clegg, W. J., Crack deflection in ceramic laminates using porous interlayers. *J. Eur. Ceram. Soc.*, 1998, **18**, 1945–1951.
4. Davis, J. B., Kristoffersson, A., Carlström, E. and Clegg, W. J., Fabrication and crack deflection in ceramic laminates with porous interlayers. *J. Am. Ceram. Soc.*, 2000, **83**(10), 2369–2374.
5. Reynaud, C., *Céramiques lamellaires monolithiques et composites en Carbure de Silicium*. Ph.D. thesis no. 282TD, Ecole des Mines, St-Etienne, France, 2002.
6. Reynaud, C., Thévenot, F., Chartier, T. and Besson, J. L., Mechanical properties and mechanical behaviour of SiC dense-porous laminates. *J. Eur. Ceram. Soc.*, 2005, **25**, 589–597.
7. Tariolle, S., Reynaud, C., Thévenot, F., Chartier, T. and Besson, J. L., Preparation and mechanical properties of SiC–SiC and B_4C–B_4C laminates. *J. Solid State Chem.*, 2004, **177**, 487–492.
8. Tariolle, S., *Carbure de Bore monolithique et poreux et composites lamellaires, élaboration, propriétés, renforcement*. Ph.D. thesis no. 328TD, Ecole des Mines, St-Etienne, France, 2004.
9. Ma, J., Wang, H., Weng, L. and Tan, G. E. B., Effect of porous interlayers on crack deflection in ceramic laminates. *J. Eur. Ceram. Soc.*, 2004, **24**, 825–831.
10. He, M. Y. and Hutchinson, J. W., Crack deflection at an interface between dissimilar elastic materials. *Int. J. Solids Struct.*, 1989, **25**(9), 153–167.
11. He, M. Y. and Hutchinson, J. W., Kinking of a crack out of an interface. *J. Appl. Mech.*, 1989, **111**, 270–278.
12. Cherti Tazi, O., Comportement à la rupture d'un assemblage de matériaux fragiles, Ph.D. thesis, University P. and M. Curie, Paris, France, 2005.
13. Leguillon, D., Strength or toughness? A criterion for crack onset at a notch. *Eur. J. Mech. A/Solids*, 2002, **21**, 61–72.
14. Leguillon, D., Sanchez-Palencia, E., *Computation of Singular Solutions in Elliptic Problems and Elasticity*. Masson, Paris, John Wiley, New York, 1987.
15. Fujita, H., Jefferson, G., McMeeking, R. M. and Zok, F. W., Mullite/alumina mixtures for use as porous matrices in oxide fiber composites. *J. Am. Ceram. Soc.*, 2004, **87**(2), 261–267.
16. Martin, E. and Leguillon, D., Energetic conditions for interfacial failure in the vicinity of a matrix crack in brittle matrix composites. *Int. J. Solids Struct.*, 2004, **41**, 6937–6948.